The whiff of decay: Linking volatile production and extracellular enzymes to outcomes of fungal interactions at different temperatures

Jade O'Leary [a], Jen Hiscox [a], Dan C. Eastwood [b], Melanie Savoury [a], Andrew Langley [a], Stuart W. McDowell [b], Hilary J. Rogers [a], Lynne Boddy [a, *], Carsten T. Müller [a]

[a] Cardiff School of Biosciences, Cardiff University, Cardiff, CF10 3AX, UK
[b] Department of Biosciences, Swansea University, Swansea, SA2 8PP, UK

ARTICLE INFO

ABSTRACT

The terrestrial carbon cycle is largely driven by photosynthetic plants and decomposer organisms that process biomass to CO_2. In forest ecosystems, the decomposers are predominantly wood decay fungi, and the response of community structure and activity to increasing global temperatures is likely critical to forest biogeochemical processes. Metabolic products can drive community structure and substrate utilisation, and the role of volatile organic compounds (VOCs), as well as extracellular enzymes, are of particular interest. Pair-wise interactions of a community of basidiomycetes were made under 3 different microclimate conditions that mimic fluctuations in local climate conditions, and the outcome of interactions was assessed in terms of: (1) which fungus won the confrontation or whether it was a draw (deadlock); (2) the production of volatile organic compounds (VOCs) and enzyme activities; and (3) the rate of decomposition. While substrate utilisation and exploitation in terms of decomposition was not affected, community response to changing temperature was underpinned by altered outcomes of interactions and changes to territory occupation, which were reflected by changes in VOC production and extracellular enzyme activity. This study underlines the importance of understanding the impact of community structure on carbon cycling in forest ecosystems under a changing climate.

1. Introduction

Sequestration of CO_2 in forest ecosystems is pivotal to the global carbon cycle. It has been estimated that between 1993 and 2003, 0.9 Pg C y^{-1} were stored within terrestrial forest sinks in soils and dead wood (Post et al., 1982; IPCC, 2007; Venugopal et al., 2016). Wood decay basidiomycetes play an essential role in these ecosystems, decomposing 120 ton km^2 y^{-1} of wood and releasing the fixed carbon and nutrients therein (White, 2003), resulting in CO_2 efflux (Cox et al., 2000). The composition of communities of wood decay fungi, and the rate at which they decompose wood, vary with temperature (Hiscox et al., 2016), and likely regulate climate feedbacks to the carbon cycle (Allison and Treseder, 2008). The average global temperature has increased by 0.8 °C since 1900 (Hansen et al., 2006) and is predicted to rise a further 1.5—2.0 °C by 2100 (IPCC, 2013), likely increasing the rate of wood decomposition (Davidson and Janssens, 2006).

Fungal communities are dynamic systems, the composition of which is constantly changing (Boddy, 2001). A high species diversity of wood decay fungi can increase the rate of decomposition (Hiscox et al., 2016; Maynard et al., 2017), especially under changing temperature regimes (Toljander et al., 2006). In the natural environment, complete wood decomposition is achieved by complex communities, rather than individual species (Boddy, 2000). During competitive interactions between these decay fungi, the activity of specific extracellular enzymes increases, as does the emission of certain volatile organic compounds (VOCs) and production of small and non-diffusible metabolites (Hynes et al., 2007; Hiscox et al., 2010, 2018; Crowther et al., 2011). In addition, the ability of wood decay fungi to produce different metabolites varies between species and individuals (Eichlerová et al., 2015), and between different combinations of fungi (Hiscox et al., 2010a).

Metabolic processes during wood decay vary depending on environmental conditions. For example, the activity of nine lignin and cellulose decomposing enzymes increased in angiosperm

---

forest soil samples as temperature increased from $-5\,°C$ to $30\,°C$, with 63—69% of the total annual enzyme activity being recorded during the warmest period of the year (Baldrian et al., 2013). The outcomes of interactions also vary with changes in temperature and historical occupancy (Hiscox et al., 2017), leading to changes in community composition and, therefore, the local enzyme pool. A direct link between activities of extracellular enzymes and interaction outcomes, however, has not to our knowledge previously been found. Environmentally induced alterations to ligninolytic/cellulolytic enzymes and VOC production during competitive interactions and the impact of these products and processes on decomposition have not even been assessed. However, in light of climate change predictions, understanding fungal interactions and changes in fungal metabolism under varied environmental conditions is crucial to fully comprehending wood decomposition processes, and how these might alter in the future.

This study investigates the relationship between changes in VOC profiles and enzyme activities in decaying wood and the outcomes of interactions between the very common and well characterised fungus *Trametes versicolor* and six other wood decay basidiomycetes under different environmental scenarios. Microclimatic effects were investigated by performing experiments in the field and at two controlled temperatures in the laboratory. Combined univariate and multivariate data analysis methods were applied to enable comparisons of individual enzyme activities, and across the whole suite of extracellular enzymes and VOCs. It was hypothesised that: (1) metabolism and interaction outcome are inherently linked, and are affected by environmental conditions; and (2) changes to metabolic strategies for antagonism and resource utilisation reflect alterations to community dynamics.

2. Materials and methods

2.1. Colonisation of wood blocks

Seven species of native, beech (*Fagus sylvatica*)-inhabiting fungi, typical of different successional stages of wood decay (Table 1), were used to colonise $30 \times 30 \times 30$ mm beech wood blocks. The blocks were sterilised by autoclaving three times for 120 min, with 48 h intervals between autoclave cycles, then placed onto 7 d old cultures of single strains on 0.5% malt agar (MA; 5 g l^{-1} malt extract, 15 g l^{-1} agar; Lab M, UK) and incubated in the dark at $20\,°C$ for 12 or 24 weeks. At the end of the pre-colonisation period, block densities were determined for each strain as dry weight/fresh volume (g cm^{-3}; 10 replicates).

2.2. Interactions set up

Blocks that had been pre-colonised for 12 weeks were scraped free of adhering mycelium 48 h before interactions were established. Immediately after scraping, marks were made on the corner of each block using a pyrography iron to indicate the identity of the strain colonising the block (Fig. 1). Blocks were paired together with cut vessels touching so that the wood grain ran in the same direction, and with markings on the corners furthest from the region of contact. They were held together using a sterile elastic band, or plastic coated garden wire (Poundland, UK) to which an aluminium forestry tag had been attached for blocks that were placed in the field. Pair-wise interactions were set up with the focal species, *T. versicolor*, against all other competitors: *Vuilleminia comedens*, *Coniophora puteana*, *Bjerkandera adusta*, *Pleurotus ostreatus*, *Hypholoma fasciculare* and *Phanerochaete velutina*. Self-pairings of all fungi were also made.

For controlled temperature experiments, blocks were placed onto perlite (30 ml; Homebase, UK) moistened with sterile distilled water to achieve a water potential of -0.012 kPa (determined by the method of Fawcett and Collins-George, 1967), in plastic 200 ml lidded pots (Cater4you, UK). A hole in the pot wall (1×2 mm diameter) covered in microporous surgical tape (3M, UK) allowed aeration. Five replicates of each pairing combination were incubated at $15\,°C$ or $25\,°C$, and were harvested 1, 14, 28, 56, and 84 d after pairings were set up.

Paired blocks were also placed in a mixed deciduous (predominantly beech) woodland site in Whitestone Woods, Tintern (lat/long 51.723105/-2.691886) (n = 5), in a 10×10 m area divided into 25 grid squares. Each grid square contained one replicate of each pairing for each sampling time point (i.e. each square contained one replicate of 16 different pairing combinations). Hourly temperature readings were taken using dataloggers distributed randomly across the site (3 replicates; TinyTag, UK; Fig. S1). Pairings were assorted randomly within each grid square and held in position with tent pegs. Five replicates of each pairing combination were collected 1, 14, 28, 56, and 84 d after interactions were established.

2.3. Sampling of VOCs

Production of VOCs was measured at $15\,°C$ and $25\,°C$ 1, 14, and 28 d after interactions between fungi in colonised wood blocks were set up. Three replicates of each pairing were chosen at random, and VOCs collected prior to block harvest and fungal re-isolation. Pots were inserted, singly and lidless, into a multi-purpose roasting bag (46×56 cm; Lakeland, UK), which was sealed and stored at $15\,°C$ or $25\,°C$ (i.e. the same as the

Table 1
Details of experimental species. Cultures were obtained from isolated mycelia from wood or fruit bodies and their identifications confirmed by ITS rRNA sequencing.

| Species	Abbreviation	Isolate ID	Provenance	Successional role	Rot type	Homo/heterokaryon
Trametes versicolor	Tv	TvAW-HxFP	Mated strain: TvAW-H with TvFP664-SSI from Clark University, MA, USA	Secondary coloniser	White	Heterokaryon
Vuilleminia comedens	Vc	VcWVJH1	Cardiff University Culture Collection	Primary coloniser	White	Heterokaryon
Coniophora puteana	Cp	Cp EMPA#62	EMPA, Switzerland	Primary coloniser	Brown	Homokaryon
Bjerkandera adusta	Ba	BaSS1	Cardiff University Culture Collection	Secondary coloniser	White	Heterokaryon
Pleurotus ostreatus	Po	Po-JWHW2014	Public University of Navarre	Secondary coloniser	White	Heterokaryon
Hypholoma fasciculare	Hf	HfGTWV2	Cardiff University Culture Collection	Late secondary coloniser/cord former	White	Heterokaryon
Phanerochaete velutina	Pv	Pv29	Cardiff University Culture Collection	Late secondary coloniser/cord former	White	Heterokaryon
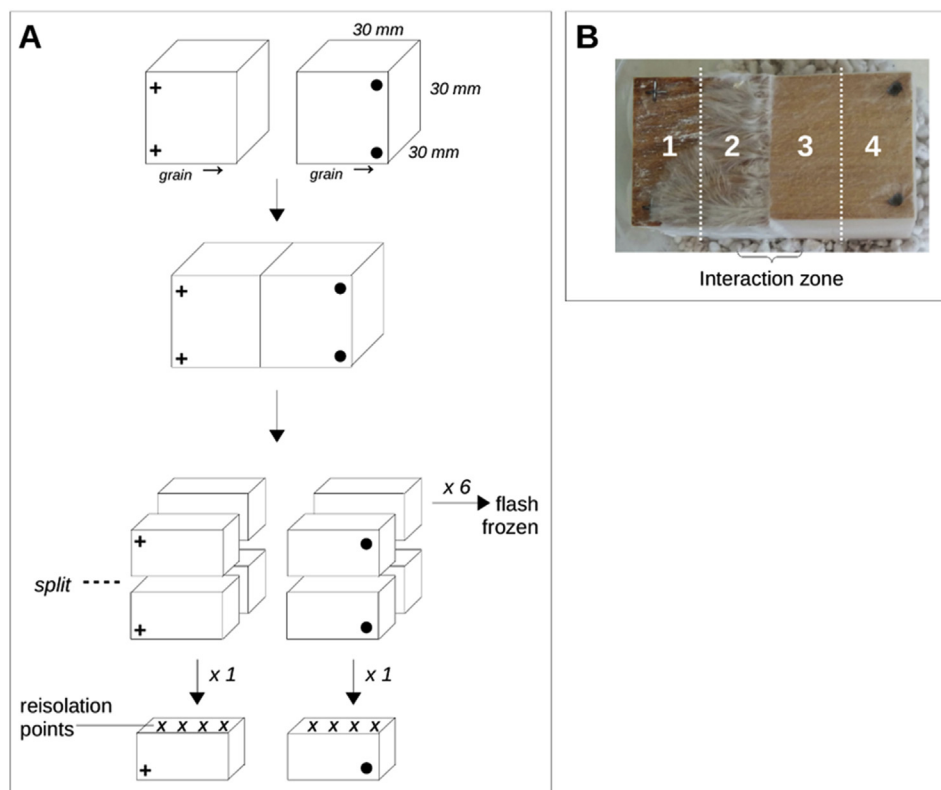
Fig. 1. Experimental set up of interactions. (A) The way in which wood blocks were paired and harvested. (B) Regions from which enzymes were extracted in interactions of *T. versicolor* with *H. fasciculare* and *P. velutina* (See Table S1 for specific details on sampled regions).

experimental incubation temperature) for 30 min to allow VOCs to equilibrate in the headspace. Headspace (500 ml) gas was collected with an EasyVOC manual pump (Markes International Ltd., UK) onto SafeLok™ thermodesorption (TD) tubes (Tenax TA & Sulficarb; Markes International Ltd., UK). Control samples comprised a pot containing uncolonised sterile beech wood blocks.

VOCs were analysed by thermodesorption time-of-flight gas chromatography-mass spectrometry (TD-TOF-GC-MS) desorbed using a TD100 thermodesorption system (Markes International Ltd.), with the following settings: tube desorption 10 min at 280 °C, at a trap flow of 40 ml min^{-1}; trap desorption and transfer 40 °C s^{-1} to 300 °C, with a split flow of 20 ml min^{-1} into gas chromatograph (GC; 7890A; Agilent Technologies Inc., Santa Clara, California, USA). VOCs were separated over 60 m, 0.32 mm I.D., 0.5 μm Rx5ms (Restek, UK) with 2 ml min^{-1} helium as carrier gas under constant flow conditions using the following temperature program: 35 °C for 5 min, 5 °C min^{-1} to 100 °C, then 15 °C to 250, final hold 5 min. Mass spectra were recorded from *m/z* 30 to 350 on a time-of-flight mass spectrometer (BenchTOF-dx, Markes International Ltd.). C8–C20 alkane standard (0.5 μl, Supelco) was loaded onto a blank thermodesorption tube as a retention standard and for quality control, (QC) and was analysed under the same conditions as samples.

2.4. VOCs data processing

Gas chromatography-mass spectrometry (GC-MS) data were processed using MSD ChemStation software (E.02.02.1177; Agilent Technologies Inc., USA) and deconvoluted and integrated with AMDIS (National Institute of Standards and Technology 11 (NIST)) using a custom retention-indexed mass spectral library. MS spectra

from deconvolution were searched against the NIST 2011 library (Software by Stein, version 2.0 g, 2011). Putative identifications were based on matches of mass spectra (>80%) and retention index (RI ± 15).

Using MetaboAnalyst 3.0 (Xia and Wishart, 2015), all data were: normalised by constant sum; g-log transformed and mean centred; missing value imputation was performed by replacement with half of the data matrix's reported minimum peak area; and inter-quantile range estimation was used to filter near-constant peaks. QCs were excluded from the matrix and the standardised binned data were used for statistical analysis.

2.5. Harvest and re-isolation procedures

For all experiments, blocks from all 5 replicates of each sample set were split into quarters using a surface-sterilised chisel (Fig. 1A). Quarters from both blocks that had been in contact in an interaction were wrapped in foil; three matched quarters were flash frozen in liquid nitrogen and stored at −80 °C, whilst the remaining quarters were used for re-isolation and density determination. For re-isolations, the quarter-blocks were split into two, and pieces of wood (~2 mm^3) excised 3.75, 11.25, 18.75 and 26.25 mm from the interaction zone. These wood chips were inoculated onto 2% MA, incubated at 20 °C and mycelia identified morphologically. The other half was used to determine final density from fresh volume and oven dry weight (g cm^{-3}) (at 84 d only), and weight loss was determined by comparison with the density of 10 blocks per species sacrificed at the start of the experiment. The rate of weight loss (mg d^{-1}) for each species was calculated as the change in block densities between the end of the pre-colonisation period (10 sacrificed blocks, described above) to interaction harvest. Using the territory

occupied by each species at the end of the experiment, the expected contribution of each species to weight loss in each interaction was calculated from the weight loss in self-pairings. These expected values were then compared with the actual weight losses determined from each block following harvest to calculate the effect of interaction processes on decomposition.

2.6. Enzyme extraction and assays

Specific interactions and regions of interactions were chosen for enzyme analysis based on the interaction outcomes determined after re-isolation onto agar. These were: (1) specific regions of blocks from interactions of *T. versicolor* with *H. fasciculare* and *P. velutina* chosen because interaction outcomes changed between different environmental conditions (see Table S1 for details of regions); and (2) all regions of interacting *T. versicolor* and *H. fasciculare* blocks over 84 d (total time taken for interaction to fully resolve). Statistical comparisons were made within these groups.

Blocks from all 5 replicates of each sample set were removed from storage at −80 °C and freeze dried for 48 h (Edwards Modulyo, UK). Sawdust was generated from blocks using a 4 mm drill bit and 0.5 g sawdust was shaken in 5 ml of 50 mM sodium acetate buffer (pH 5.0) at 4 °C overnight. The activities of the following terminal hydrolases were measured using 4-methylumbelliferol (MUF)-based substrates as described previously (Baldrian, 2009; Šnajdr et al., 2011): β-glucosidase (EC 3.2.1.21), α-glucosidase (EC 3.2.1.20), cellobiohydrolase (EC 3.2.1.91), β-xylosidase (EC 3.2.1.37), exochitinase (EC 3.2.1.201), phosphodiesterase (EC 3.1.4.1), phosphomonoesterase (EC 3.1.3.2) and arylsulfatase (EC 3.1.6.1). Briefly, substrates (40 μl in dimethylsulphoxide) at final concentration of 500 mM were combined with three technical replicates of 200 μL of samples (diluted 1:10) in a 96 well plate. Background fluorescence was determined by combining 200 μL sample (diluted 1:10) with 40 μl MUF standards. The 96 well plates were incubated at 40 °C and fluorescence recorded at 5 and 125 min using a Tecan Infinite microplate reader (Tecan, Männedorf, Switzerland) with an excitation wavelength of 355 nm and an emission wavelength of 460 nm. Quantitative enzymatic activities were calculated after blank subtraction based on a standard curve of MUF. One unit of enzyme activity was defined as the amount of enzyme releasing 1 mM of MUF min^{-1}.

Laccase (phenoloxidase; EC 1.10.3.2) activity was determined by quantifying the oxidation of 2,2′-azino-bis(3-ethylbenzothiazoline-6-sulfonic acid) diammonium salt (ABTS) in citrate-phosphate buffer (100 mM citrate, 200 mM phosphate, pH 5.0; according to Bourbonnais & Paice 1990), by quantifying the formation of green colouration spectrophotometrically at 420 nm. Three technical replicates were performed for each sample.

Manganese peroxidase (MnP; EC 1.11.1.13) activity was determined by monitoring spectrophotometrically at 595 nm the purple colouration from oxidative coupling of 3-methyl 2-benzothialone-hydrazone hydrochloride (MBTH) and 3-(dimethyl amino)-benzoic acid (DMAB) in succinate-lactate buffer (100 mM, pH 4.5). Three technical replicates were performed for each sample. The assay was repeated with ethylene diamine tetraacetate (EDTA) to chelate any Mn^{2+} present in the samples, allowing detection of Mn^{2+}-independent peroxidases (versatile peroxidase), and the results of the MnP assay were corrected using activities of samples without manganese. The results were also corrected using activities of samples in a separate version of the assay in the absence of H$_2$O$_2$, allowing detection of oxidase (but not peroxidase) activity.

Activities of enzymes within a sample were normalised to the protein content of that sample, determined using Qubit™ fluorometric assays (ThermoFisher Scientific Inc., Loughborough, UK).

2.7. Statistical analysis

Principal component analysis (PCA) was used to check the unsupervised segregation of the entire GC-MS data set and clustering of the QCs (see Fig. S2), in Metaboanalyst 3.0 (Xia and Wishart, 2015). QCs were deemed as sufficient quality and were removed from the data set. Differences between VOC profiles were assessed using permutational multivariate analysis of variance (PerMANOVA) in the 'vegan' package (Oksanen et al., 2013) in R statistical software (R Core Team, 2014). Orthogonal projection to latent structures-discriminant analysis (OPLS-DA) was then applied to each sample group separately: 15 °C and 25 °C (i.e. 2 OPLS-DA models), and to each time point for each sample group (i.e. 6 OPLS-DA models) in Metaboanalyst 3.0. Compounds contributing most to fluctuation in the discriminant models were identified from the modelled covariance and correlation. Then, univariate one-way analysis of variance (ANOVA) with a 5% Benjamini-Hochberg false discovery rate (FDR) correction for multiple comparisons (Benjamini and Hochberg, 1995) was applied to significant compounds, with Tukey *Post-hoc* tests.

The actual and expected weight losses following interaction harvest were compared using a one-way *t*-test (where the hypothesis was that there was no significant difference to 0), conducted in R.

Differences between enzyme profiles were assessed using PerMANOVA and canonical analysis of principal coordinates (CAP) Anderson and Willis (2003) in the 'vegan' (Oksanen et al., 2013) and 'BiodiversityR' packages (Kindt and Coe, 2005) in R. Ordination plots were generated from CAP and a 95% confidence interval was fitted. Following CAP, weighted correlation network analysis (WCNA) (Langfelder and Horvath, 2012) was applied to identify sub-sets of enzymes differentially correlated with time of sampling, environmental condition and pairing combination. OPLS-DA was conducted in Metaboanlyst 3.0 to confirm the results from CAP and WCNA. Additionally, activities of individual enzymes (mean of 5 replicates) were compared using one-way ANOVA in combination with Tukey *post hoc* tests when data were normally distributed, or Kruskal-Wallis tests followed by a Dunn's test *post hoc* procedure when data were non-normally distributed, in R statistical software.

3. Results

3.1. Interaction outcomes change under different abiotic regimes

Generally, the combative ability of *T. versicolor* increased with temperature, and in some cases interaction outcomes were reversed under the different temperature regimes (Fig. 2). For example, *T. versicolor* was partially replaced by *H. fasciculare* and *P. velutina* at 15 °C, but at 25 °C it deadlocked with *H. fasciculare* and partially replaced it in some replicates, and fully replaced *P. velutina*. *T. versicolor* only partially replaced *V. comedens* and *P. ostreatus* at 15 °C but fully replaced both at 25 °C (Fig. 2). Additionally, under field conditions where temperature varied with an average of 12 °C over the experimental period (Fig. S1), *T. versicolor* was less combative against *V. comedens*, *P. ostreatus* and *P. velutina* compared to when interacting at higher temperatures in the laboratory. When against *C. puteana* and *H. fasciculare* under field conditions, however, *T. versicolor* was marginally more combative than when interacting at 15 °C, and the interaction of *T. versicolor* against *B. adusta* was not affected by field conditions.

3.2. Profiles of volatile organic compounds vary depending on temperature, pairing combination and time

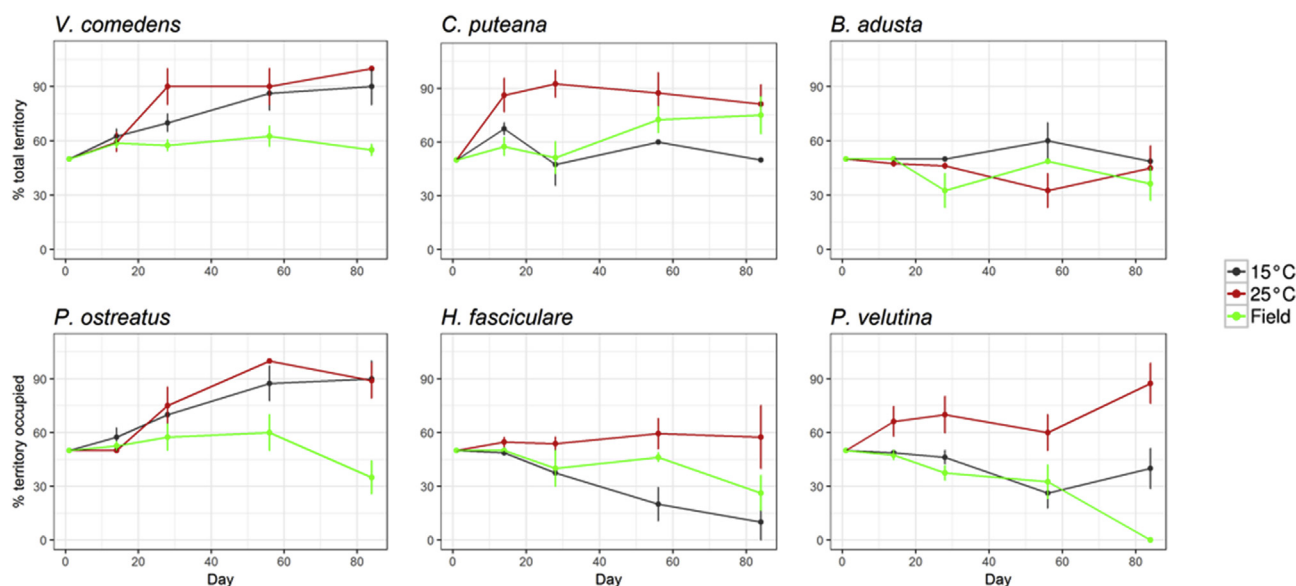After noise reduction, overall a total of 72 compounds were

Fig. 2. Percentage territory of resource occupied by *T. versicolor* throughout the duration of the interaction period (84 d). Species names indicate interaction competitor.

detected, 63 of which were putatively identified by comparison to the NIST library of mass spectra (Table 2). Compound classes included sesquiterpenes (16), alkanes (14), esters (9), ketones (6), alkenes (6), alcohols (4), aldehydes (3), monoterpenes (1), terphenyls (1), amides (1), ethers (1), and alkenols (1). Bouquet composition was significantly dependent on temperature (PerMANOVA, $p < 0.001$, $R^2 = 0.051$), the combination of species pairings ($p < 0.001$, $R^2 = 0.133$), and the time for which fungi had been paired ($p < 0.001$, $R^2 = 0.114$), accounting for 30% of the total variance.

At 15 °C, a total of 57 VOCs were detected (Table S2A) and the supervised OPLS-DA scores plot showed separation between the three sampling times accounting for 20% of the variance (T score [1] axis; Fig. 3A), with profiles of interactions after 1 d and 28 d being significantly different while VOC profiles of interactions after 14 d overlapped with the other two time points. The greatest degree of separation occurred between different interactions (Fig. 3B–D). VOC profiles of individual pairings at 15 °C were most distinct from each other after 14 d, with *V. comedens* self-pairings and interactions between *T. versicolor* and *B. adusta* distinctly separating from any other interactions (Fig. 3C). At 25 °C, 47 compounds were detected, 10 less than at 15 °C (Table S2B). Again, profiles of individual pairings changed over time (orthogonal T score [1] axis: 41% of the variance; Fig. 3E). VOC profiles of some interactions were discriminated from all others: for example *T. versicolor* against *V. comedens*, and *C. puteana* and *P. ostreatus* self-pairings after 28 d (Fig. 3H). Compounds contributing significantly to group separation at 15 °C and 25 °C are listed in Table S3 and Table S4 respectively.

At both temperatures, many compounds were produced *de novo* during competitive interactions compared to control self-pairings, and some which were produced in self-pairings were not produced during interactions. For example, 2-ethyl-4-methyl-1-pentanol (C12) was produced when *T. versicolor* was interacting with *P. ostreatus* at 15 °C and with *C. puteana* at 25 °C, but was not produced in self-pairings of any of those fungi (Table S2). Additionally, the abundance of many compounds was reduced or increased in interspecific interactions compared to self-pairings and could be linked to interaction outcomes, e.g., the abundance of 2-ethylhexyl trans-4-methoxycinnamate (C19) was reduced across all time points when *T. versicolor* was partially replaced by

B. adusta at 25 °C, but its abundance increased at all time points when *T. versicolor* partially replaced *C. puteana* at 25 °C (Table S2).

3.3. Rate of decay is largely unaffected by interaction processes

Decay rate was not significantly different ($p > 0.05$) from what was expected, based on the rate of decay of respective self-pairings, in almost all interspecific interactions (Fig. 4). The exception to this was the interaction between *T. versicolor* and *P. velutina* at 25 °C which resulted in partial replacement of *P. velutina*, which lost significantly more weight than was estimated, based on when the fungi were growing in monocultures (Fig. 4).

Extracellular enzymes function independently from each other, and activity reflects interaction outcomes and different environmental condition.

Enzyme profiles of interactions whose outcome changed as a result of abiotic condition were significantly different amongst temperature (PerMANOVA, $p < 0.01$, $R^2 = 0.045$) and species combinations ($p < 0.05$, $R^2 = 0.051$), but this only accounted for 1% of the variance. Significant differences were confirmed by CAP but there was no clear separation between abiotic condition (percentage of correct classification of 60.95% at $p < 0.005$), nor between species combination (59.73% at $p < 0.005$) (Fig. 5A and B). WCNA clustered the analysis parameters into a single module, indicating that there was no correlation between enzyme profiles, pairing combination, abiotic condition nor interaction outcome. OPLS-DA confirmed the lack of discrimination between group enzymatic profiles (Figs. S3A and B), despite individual enzymes being significantly associated with group clusters (ANOVA: $p < 0.05$).

Treating each enzyme independently to each other, i.e. not as a profile, showed that activity of individual enzymes was significantly associated with interaction outcome. For example, the activity of β-glucosidase was significantly higher (ANOVA: $p < 0.05$) in the interaction zone when *T. versicolor* deadlocked with competitors at 15 °C compared to when it was replaced (either partially or fully) by *H. fasciculare*. β-glucosidase was similarly significantly higher during deadlock compared to a partial replacement of *H. fasciculare* and *P. velutina* by *T. versicolor* at 25 °C (Table 3). For both interactions tested (*T. versicolor* against *H. fasciculare* and *P. velutina*), different outcomes were associated with significantly

Table 2
VOC compounds putatively identified by TD-TOF-GC-MS. Retention index (RI), CAS registry number, chemical group and reference of previous reporting of presence in a fungal or microbial system are given.

|	Compound name	RI	CAS	Chemical group	Reference
C1	4-epi-α-Acoradiene	1474	729602-94-2	Sesquiterpene	
C2	β-Alaskene	1502.7	99529-78-9	Sesquiterpene	
C3	α-Barbatene	1415.5	53060-59-6	Sesquiterpene	
C4	β-Barbatene	1441	72346-55-5	Sesquiterpene	
C5	Azulene	1532.2	395070-76-5	Sesquiterpene	
C6	[1,1':3′,1"-Terphenyl]-2′-ol	2275	2432-11-3	Terphenyl	
C7	Phthalic acid	2299	84-64-0	Aldehyde	Yan et al. (2008)
C8	(+)-Sativen	1396.2	3650-28-0	Sesquiterpene	Savel'eva et al. (2014)
C9	1-Dodecanone, 2-(imidazole-1-yl)-1-(4-methoxyphenyl)-	2742	2432-11-3	Ketone	
C10	2-Methyl-1-heptene	782	15870-10-7	Alkene	Schalchli et al. (2011)
C11	2-Butyl-1-octanol	1277	3913-02-8	Alcohol	
C12	2-Ethyl-4-methyl-1-pentanol	931	106-67-2	Alcohol	
C13	1S-a-Pinene	942	7785-26-4	Monoterpene	Rivas da Silva et al., 2012
C14	2,4-Dimethyl-1-heptene	819	19549-87-2	Alkene	Cordero et al., 2015; Suwannarach et al., (2016)
C15	2,4-Dimethyl-1-hexene	720	16746-87-5	Alkene	
C16	2-Butanone	555	78-93-3	Ketone	Isidorov et al. (2016)
C17	3-Methyl-2-butanone	590	563-80-4	Ketone	Konuma et al., 2015; Savel'eva et al., 2014
C18	(Z)-6-methyl-2-decene	1059	74630-31-2	Alkene	
C19	2-Ethylhexyl trans-4-methoxycinnamate	2322	83834-59-7	Ester	Fernandez de Simon et al. (2014)
C20	2-Propenoic acid ester 1	2188	5466-77-3	Ester	
C21	2-Propenoic acid ester 2	2336	5466-77-3	Ester	
C22	3-Octanone	966	106-68-3	Ketone	Isidorov et al. (2016)
C23	3-Pentanol	681	584-02-1	Alcohol	Wihlborg et al. (2016)
C24	β-Patchoulene	1356	514-51-2	Sesquiterpene	
C25	5,5-Dimethyl-1,3-hexadiene	730	1515-79-3	Alkene	
C26	Methyl acetate	487	79-20-9	Ester	Sharip et al. (2016)
C27	Acetone	455	67-64-1	Ketone	Isidorov et al. (2016)
C28	α-Longipinene	1422	59-89-08-2	Sesquiterpene	Isidorov et al. (2016)
C29	Cuparene	1556	16982-00-6	Sesquiterpene derivative	Konuma et al. (2015)
C31	Isocaryophyllene	1434	118-65-0	Sesquiterpene	Sánchez-Fernández et al. (2016)
C32	Unknown1	1026	–	–	
C33	Unknown2	1312	–	–	
C34	Unknown3	1084	–	–	
C35	Unknown4	1235	–	–	
C36	Unknown5	1245	–	–	
C37	Unknown6	1250	–	–	
C38	Cedrene	1403	469-61-4	Sesquiterpene	Konuma et al. (2015)
C39	Cetene	1889	629-73-2	Alkene	Konayli et al., (2009); Usha Nandhini et al., (2015)
C40	cis-Thujopsene	1454	470-40-6	Sesquiterpene	Konuma et al. (2015)
C41	Decanal	1186	112-31-2	Ketone	Ho et al. (2010)
C42	2,9-Dimethyldecane	1086	1002-17-1	Alkane	
C43	4,6-Dimethyldodecane	1285	61141-72-8	Alkane	Geethalakshmi and Sarada (2013)
C44	Methylformamide	607	123-39-7	Amide	Chen et al. (1989)
C45	2,3-Dimethylheptane	788	3074-71-3	Alkane	
C46	4-Methylheptane	752	589-53-7	Alkane	Sinha et al. (2015)
C47	5-Ethyl-2-methylheptane	887	13475-78-0	Alkane	Zerinque and Bhatnagar (1994)
C48	Hexadecanoic acid, methyl ester	1878	112-39-0	Ester	Kong et al. (2004)
C49	2,3,5-Trimethylhexane	724	1069-53-0	Alkane	Borjesson et al. (1989)
C50	Isopropyl palmitate	2013	110-27-0	Ester	Pan et al. (2016)
C51	Longifolene	1428	475-20-7	Sesquiterpene	Konuma et al. (2015)
C52	1-Heptadecanol	1954	1454-85-9	Alcohol	Qadri et al. (2017)
C53	2,5-Dimethylnonane	1027	17302-27-1	Alkane	Lippolis et al. (2014)
C54	Octyl ether	1665	629-82-3	Ether	Pernak et al. (2004)
C55	2,7-Dimethyloctane	933	1072-16-8	Alkane	Schaeffer et al. (1979)
C56	4-Methyloctane	872	2216-34-4	Alkane	Ahearn et al. (1997)
C57	6-ethyl-2-methyloctane	1158	62016-19-7	Alkane	Sen et al. (2017)
C58	β-Chamigrene	1504	18431-82-8	Sesquiterpene	Mun and Prewitt (2011)
C59	α-Chamigrene	1533	19912-83-5	Sesquiterpene	Mun and Prewitt (2011)
C60	4,8-Dimethylundecane	1218	17301-33-6	Alkane	
C61	Unknown7	1161	–	–	
C62	Butyl 2-ethylhexyl phthalate	2370	85-69-8	Aldehyde	Sun et al. (2015)
C63	6-Methyl-5-hepten-2-ol	964	1569-60-4	Alkenol (aliphatic alkenone)	Liouane et al. (2010)
C64	Benzoic acid ester	2392	–	Ester	
C65	Benzoic acid, tridecyl ester	2300	–	Ester	
C66	Unknown8	900	–	–	
C67	Unknown9	695	–	–	
C68	2,5-Dimethylhexane	688	592-13-2	Alkane	Micheluz et al. (2016)
C69	γ-Cadinene	1538	39029-41-9	Sesquiterpene	Konuma et al. (2015)
C70	Palmitic acid	1968	57-10-3	Aldehyde	Gutierrez et al. (2002)
C71	3,6-Dimethyloctane	940	15869-94-0	Alkane	
C72	2,8-Dimethylundecane	1225	17301-25-6	Alkane	
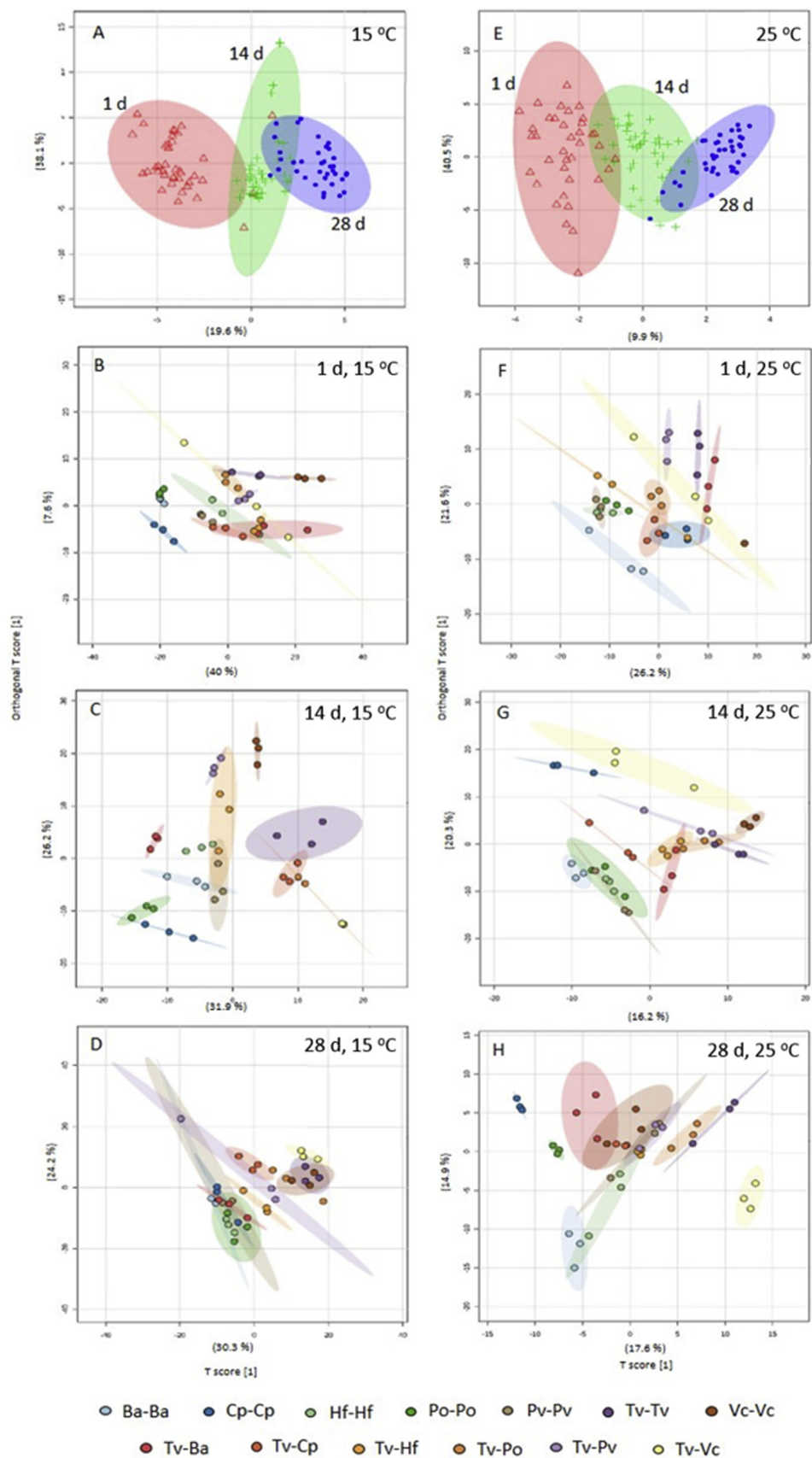
Fig. 3. OPLS-DA scores plots derived from the GC-MS spectra of interactions at 15 °C (A—D) and 25 °C (E—H). (A,E) Samples from all three time classes, individual pairings (B,F) 1 d after interaction set up, (C,G) after 14 d, and (D,H) after 28 d. Points represent individual samples (three independent biological replicates per pairing), and 95% confidence intervals of the means of sample groups are fitted onto the spatial ordination. Ba: *B. adusta*, Cp: *C. puteana*, Hf: *H. fasciculare*, Po: *P. ostreatus*, Pv: *P. velutina*, Tv: *T. versicolor*, Vc: *V. comedens*.
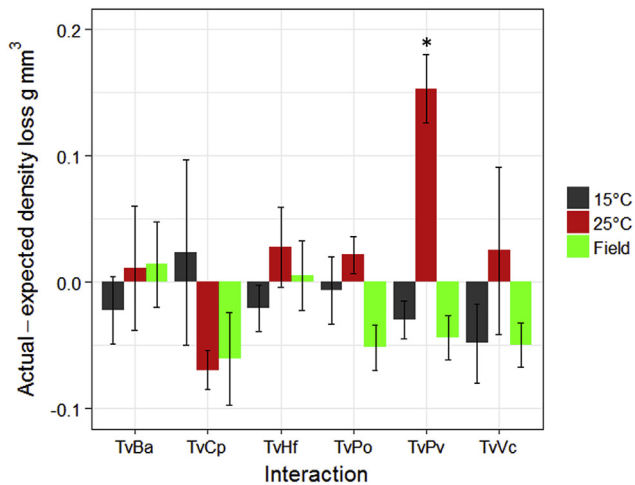
Fig. 4. Changes in block density (g mm^3) following interactions (n = 5). The bars represent replicate mean ± 95% confidence interval. * indicates actual density loss minus estimated density loss (based on the rate of decay of self-pairings) was significantly (one-way t-test: $p < 0.05$) different to 0.

different MnP activity, except when *T. versicolor* and *H. fasciculare* interacted in the field (Table 3; Fig. S4). Conversely, there was little or no MnP activity when *T. versicolor* and *P. velutina* were in deadlock, whether early or late in the interaction process, but activity significantly increased when a competitor was partially replaced at 15 °C and 25 °C.

Abiotic conditions altered the activity of individual enzymes between identical pairings with the same outcomes, and usually activity was greatest at a lower temperature. For example, α-glucosidase, β-glucosidase and phosphodiesterase activity was greatest in field samples that resulted in partial replacement of *T. versicolor* by *H. fasciculare*, compared to samples where *T. versicolor* was also partially replaced by *H. fasciculare* at 15 °C

(Table 3A,C; Fig. S4). Additionally, changes in interaction outcome at different temperatures were reflected by changes in enzyme activity, e.g. β-glucosidase activity was significantly higher ($p < 0.05$) when *H. fasiculare* partially replaced *T. versicolor* at 15 °C, compared to when *H. fasiculare* was partially replaced in the same interaction at 25 °C (Table 3A,B; Fig. S4).

3.4. Enzyme activity is correlated with territory occupation changes over time

During the interaction between *T. versicolor* and *H. fasciculare* which was tracked for 84 d, PerMANOVA revealed significant differences in enzyme profiles between sampling times ($p < 0.001$, R^2 = 0.095), and the region of interaction assayed (i.e. *T. versicolor* and *H. fasciculare* self-pairing interaction zones, and the *T. versicolor* or *H. fasciculare* colonised side of the interspecific pairing; $p < 0.001$, R^2 = 0.403), accounting for 50% of the overall variance. As before, CAP confirmed significant differences ($p < 0.05$) between profiles of enzymes, although clear separation between sampling times and interaction region were not observed (percentage of correct classi-fication of 57.86% and 65.71% respectively) (Fig. 5C and D), WCNA and OPLS-DA failed to detect correlation between enzyme profiles and sampling time nor interaction region (Figs. S3C and D).

When analysed at an individual level, significant differences in activity between groups were revealed, e.g. the activity of seven enzymes in the *T. versicolor* side of the interaction zone and eight enzymes on the *H. fasciculare* side significantly changed over time (Table 4; Fig. S5). Acid phosphatase, the most active enzyme during this interaction, was linked to *T. versicolor* as it was produced in high abundance, relative to other enzymes, in the *T. versicolor* side of the interaction zone, whereas activity on the *H. fasciculare* side of the interaction was significantly lower (ANOVA: $p < 0.05$). Inter-estingly, it increased at 14 d, when *H. fasciculare* began the process of replacement of *T. versicolor* (Fig. 3B), before returning to pre-interaction levels by 28 d. Further, β-glucosidase activity in the *H. fasciculare* side of the interaction zone was greatest at 14 d, and
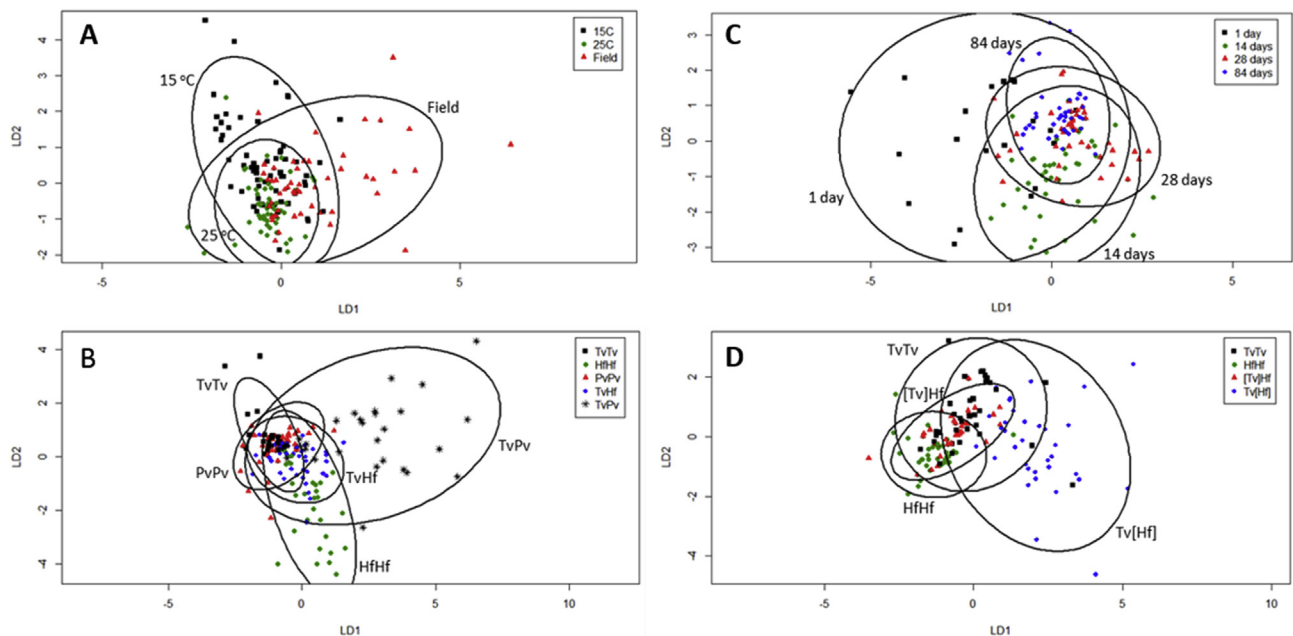

Fig. 5. Canonical analysis of principal coordinates (CAP) plots using the average activity (n = 5) of enzyme profiles. CAP models were produced for (A) abiotic condition and (B) interaction combination for interactions whose outcomes differed between 15 °C, 25 °C and field site conditions, and for (C) sampling time and (D) region of interactions assayed for the interaction between *T. versicolor* and *H. fasiculare* over 84 d (where square brackets indicate side of the interaction zone). Ellipses show 95% confidence interval and the first two linear discriminants (LD) are shown. Tv, *T. versicolor*; Hf, *H. fasciculare*; Pv, *P. velutina*.

Table 3

Enzyme activity in interactions with *T. versicolor* against *H. fasciculare* and *P. velutina*. Different outcomes occurred as interactions progressed and specific replicates were sampled accordingly (see Table S1 for details). (A) Activity in the 15 °C experiment. (B) Activity in the 25 °C experiment. (C) Activity under field conditions. Values are means of 5 replicates. ‡ Significant difference ($p < 0.05$) in activity compared with corresponding interaction at 15 °C. φ Significant difference ($p < 0.05$) in activity compared with corresponding interaction at 25 °C. Ω Significant difference ($p < 0.05$) in activity compared with corresponding interaction under field conditions. (−) represents a failed assay.

A: at 15 °C	Activity mU g^{-1}											
	Hf—Hf		Pv—Pv		Tv—Tv		Tv—Hf			Tv—Pv		
	Initial	Late	Initial	Late	Initial	Late	Initial deadlock	PR of Tv	R of Tv	Initial deadlock	PR of Tv	Late deadlock
Laccase	0.02	0.00	1.22 φΩ	1.05 φΩ	1.53 a	0.00 b	1.84	7.25	1.79	0.00 a	10.37 bΩ	0.26 a
MnP	5.85	21.20	15.69	15.79 Ω	7.82 Ω	3.08	0.00 a	13.77 b	9.18 ab	0.00 a	26.00 b	0.00 a
Peroxidase	1.22	24.80 φ	3.19 Ω	—	0.00	28.74	2.53	2.99	0.00	0.98	4.83	0.00
α-glucosidase	0.00 Ω	0.00	5.82	14.47 φΩ	43.69 φ	63.25	0.00 Ω	1.34 Ω	6.28	10.67 b	41.90 a	8.53 b
Cellobiohydrolase	0.00 Ω	0.00	0.00 a	16.98 b	7.75 φ	0.00 Ω	8.38	11.81	0.00 a	20.89 b	0.00 a
β-glucosidase	30.58	2.12 φΩ	71.34	0.38 φΩ	271.40	121.07	119.95 a	26.07 b φΩ	45.02 b	149.10 a φΩ	29.83 bΩ	145.97 a
Exochitinase	32.32	16.64	9.23	19.70 Ω	40.81 φ	27.83	29.15 φ	16.16	26.26	23.31 ab φ	62.58 a	11.46 b
Acid phosphatase	88.73 φ	68.78 Ω	979.04	1698.41 Ω	1339.15 φ	1711.30	332.30 φ	198.16	274.22	510.29 φ	806.31	423.92
Phosphodiesterase	1.16	0.00 Ω	56.78 φ	82.72 φΩ	84.41 φ	91.32	14.05 φ	0.00 Ω	0.82	25.32 φ	21.31	33.86
Arylsulfatase	0.00	9.11	9.27	14.59	0.00	0.00	0.00	3.58	4.00	9.08	4.03	3.05
β-xylosidase	70.00 a	0.00 bΩ	0.00	6.42 φ	37.56	15.09	10.60 φ	7.87	12.14	1.62 a	16.82 b	1.85 a
Oxidase	0.83	0.00	4.83	23.40	10.78	0.00	0.14	0.95	8.26	0.00	3.32	4.34

B: at 25 °C	Activity mU g^{-1}											
	Hf—Hf		Pv—Pv		Tv—Tv		Tv—Hf			Tv—Pv		
	Initial	Late	Initial	Late	Initial	Late	Initial deadlock	PR of Hf	Late deadlock	Initial deadlock	PR of PV	R of PV
Laccase	0.00	0.00	0.00 ‡	0.00 ‡	0.00	2.30 Ω	19.42 Ω	17.22	0.34	2.19 Ω	4.36	5.06
MnP	1.52	3.11	1.04	2.45 Ω	4.43	2.68	2.01 a	0.65 ab	0.00 b	0.00 a	11.20 b	0.53 a
Peroxidase	1.83 a Ω	0.00 b ‡	0.77 Ω	0.00	0.48	0.00	0.90 a	0.03 ab	4.92 b	1.74	0.00	0.61
α-glucosidase	0.00	0.00	0.53	3.36 ‡	1.10 ‡Ω	38.88	0.76	0.00	0.00 Ω	0.00	0.00	0.00
Cellobiohydrolase	0.00 Ω	0.00	0.00	2.75	0.00 Ω	0.00 Ω	0.00	0.00	3.40	0.00	0.00	0.00
β-glucosidase	13.15	12.15 ‡	51.25	112.23 ‡	76.53	100.94	57.20 ab ‡	8.71 a ‡	86.32 b	42.567 a ‡	12.47 b	35.03 ab
Exochitinase	7.70	5.11	3.36 a Ω	11.13 b	6.07 ‡Ω	17.41	7.74 ‡	2.83	4.42 Ω	1.38 ‡Ω	0.00	2.32
Acid phosphatase	33.24 ‡Ω	43.74 Ω	408.72	1280.09	390.75 ‡Ω	1061.02	106.41 a Ω	35.46 b	51.19 ab Ω	88.63 ‡Ω	65.31	73.35
Phosphodiesterase	0.00	0.00 Ω	15.58 ‡	47.98 ‡Ω	11.27 ‡Ω	82.65	1.13 ‡Ω	0.51	0.07	4.94 ‡Ω	1.44	0.85
Arylsulfatase	0.00	0.00	5.41	0.00	—	14.39	0.00	1.66	0.38	4.05	0.00	0.00
β-xylosidase	0.83	0.00	0.18	0.00 ‡	0.00 a	9.28 b	2.82 a ‡	0.00 b	0.00 b Ω	0.00 Ω	0.00	0.00
Oxidase	1.98	1.61	1.00	0.16	3.52	2.91	7.11	9.86	0.00	0.08	4.21	6.01

C: in the field	Hf—Hf		Pv—Pv		Tv—Tv		Tv—Hf			Tv—Pv		
	Initial	Late	Initial	Late	Initial	Late	Initial deadlock	PR of Tv	Late deadlock	Initial deadlock	PR of Tv	R of Tv
Laccase	0.00	—	0.00 ‡	0.00 ‡	0.00	0.00 φ	4.25 a φ	2.10 ab	0.00 b	0.00 φ	0.00 ‡	3.57
MnP	1.12	—	3.23 a	0.00 b ‡φ	0.00 ‡	2.88	3.42	5.38	2.47	3.50 a	5.17 ab	12.00 b
Peroxidase	1.24 φ	51.77	0.00 ‡φ	0.00	8.69	0.00	1.17 a	3.51 ab	0.00 b	2.23 ab	9.79 a	4.34 b
α-glucosidase	0.28 ‡	—	5.63	2.39 ‡	129.70 φ	94.66	7.69 ‡	21.30 ‡	19.14 φ	19.75	60.01	48.29
Cellobiohydrolase	0.00 ‡φ	−32.13	4.18	4.16	20.97 φ	26.92 ‡φ	0.59	3.13	5.79	7.35	10.49	7.66
β-glucosidase	15.36	291.74 ‡	114.19	76.59 φ	270.11	282.49	105.54	124.65 ‡	152.81	185.23 ‡	235.37 ‡	162.92
Exochitinase	17.07	101.89	13.70 φ	11.80 ‡	75.50 φ	55.43	18.57	45.70	34.43 φ	28.54 φ	116.44	74.97
Acid phosphatase	174.03 φ	4909.68 ‡φ	975.51	951.24 ‡	1830.82 φ	936.01	344.51 φ	322.27	248.73 φ	779.66 φ	1679.15	1437.30
Phosphodiesterase	3.58 a	66.92 b ‡φ	41.41	20.08 ‡φ	77.23 φ	76.91	12.58 φ	10.61 ‡	6.19	25.02 φ	33.88	31.22
Arylsulfatase	0.00	—	0.00	0.00	0.00	0.00	0.00	—	0.00	0.00	—	0.00
β-xylosidase	6.59	85.34 ‡	2.12	1.99	39.02	28.22	7.66	8.47	11.97 φ	13.78 φ	17.94	10.15
Oxidase	0.84	0.00	1.07	0.97	2.43	3.25	2.81	2.19	0.61	0.00	0.00	2.16

α-glucosidase was only produced by *H. fasciculare* at 14 d (Table 4; Fig. S5).

4. Discussion

This study elucidates the relationship between wood decay and metabolism by interacting fungi, and the stability of that relationship under environmental change by assessing interactions of a community of fungi in their natural substratum, wood. Abiotic conditions, specifically temperature, caused the outcome of interspecific interactions in wood blocks to change, and different outcomes were reflected by changes to substrate utilisation and metabolism.

4.1. Reversal of outcomes at different temperatures is reflected by metabolite production

Changes to the relative combative ability of wood decay fungi and reversal of outcomes under different temperature regimes have been reported previously (Hiscox et al., 2016), and may be attributed to the different temperature optima for growth of individual competitors. A previous study found no link between the activity of wood decay-associated enzymes and differences in interaction outcome (Hiscox et al., 2010). However, in that study, the different outcomes examined arose from combinations of different competitors, rather than from the same pair of competitors under different conditions, the latter being the case in the present study. Crucially, we found changes to enzyme activity and VOC production in self-pairings under different environmental conditions in the present study, suggesting that metabolic changes are temperature-induced, as has been shown previously in the fungal proteome (Moody et al., 2018). Generally, more VOCs were detected and individual enzymes were usually more active at the lower temperature. For example, 1S-α-pinene (C13), a monoterpene with known antimicrobial activity against *Candida albicans* (Rivas da Silva et al., 2012), was not detected in any pairing at 25 °C but was detected in 12 of the 13 pairings at 15 °C. The outcomes of

Table 4

Enzyme activity in both the interaction zone, and non-interaction region of *T. versicolor* (Tv) and *H. fasciculare* (Hf) blocks at 1, 14, 28 and 84 d under 15 °C controlled temperature. Values are means of 5 replicates. ‡ Significant difference ($p < 0.05$) in activity compared with additional region of block (interaction zone (IZ) − non-interaction region (Non-IZ)). ϕ Significant difference ($p < 0.05$) in activity compared with competitor side of the interaction zone. Square bracket indicates side of the interaction zone sampled. (−) represents a failed assay.

	Activity mU g⁻¹													
	Tv–Tv							Hf–Hf						
	IZ				Non-IZ			IZ				Non-IZ		
	1 d	14 d	28 d	84 d	14 d	28 d	84 d	1 d	14 d	28 d	84 d	14 d	28 d	84 d
Laccase	30.10 a	8.85 ab	12.82 ab	2.92 b	13.76 a	14.87 ab	1.87 b	15.30 a	0.00 b	47.02 a	0.50 b	1.43	14.61	21.86
MnP	21.40	14.47	24.25	13.67	17.79	14.79	11.45	6.37	3.83	8.67	2.14	4.59	5.64	0.00
Peroxidase	2.64	0.44	0.00	0.61	0.00	1.03	1.32	0.85	1.64	2.57	0.00	4.46	2.45	1.15
α-glucosidase	212.51	81.78	94.13	111.62	75.00	98.50	111.33	5.49	0.17	0.00	0.00	0.00	0.00	0.00
Cellobiohydrolase	65.00	57.90	15.79	11.28	44.26	23.55	13.75	0.85	0.36	0.00	0.00	0.00	0.00	0.00
β-glucosidase	1201.84	1193.52	602.23	441.01	978.71	635.96	522.27	213.42	89.43	85.33	61.85	108.61	105.59	70.01
Exochitinase	120.48	62.19	60.93	47.75	56.55	57.49	42.37	46.71	57.28	36.28	32.07	54.22	39.68	32.96
Acid phosphatase	3081.74	1615.79	1804.10	2062.95	1350.40	1598.02	2010.78	549.18	159.00	151.86	225.14	158.69	160.70	210.21
Phosphodiesterase	174.80	131.61	117.89	114.57	128.57	102.12	105.64	18.57	11.14	3.46	6.29	8.34	7.06	9.26
Arylsulfatase	−	5.89 ab	241.78 b	17.57 b	42.45	67.51	−	113.40	−	−	35.23	117.00	32.03	20.59
β-xylosidase	92.37 a	60.54 ab	33.59 b	29.83 b	58.95	34.55	30.62	28.73	31.22	14.67	13.27	30.25	21.59	15.65

	Activity mU g⁻¹													
	[Tv]–Hf							Tv–[Hf]						
	IZ				Non-IZ			IZ				Non-IZ		
	1 d	14 d	28 d	84 d	14 d	28 d	84 d	1 d	14 d	28 d	84 d	14 d	28 d	84 d
Laccase	79.93 a	41.06 ab	28.81 ab ‡ϕ	24.03 b	14.69	6.04 ‡	7.20	18.13 a	19.70 ab	6.33 ab ϕ	3.74 b	4.66	21.33	9.13
MnP	22.35	10.68	11.05	9.16	8.23	23.61	5.01	11.86 a	8.19 ab	30.56 ab	2.07 b	7.23	34.90	2.42
Peroxidase	10.46 a	5.59 ab	5.42 ab	2.40 b	0.71	6.57	4.80	12.76 a	4.16 ab	1.66 bc	0.00 c	3.17	0.94	0.02
α-glucosidase	103.40 ϕ	24.01	17.86	0.00	18.66	24.58	0.00	0.00 ϕ	20.62	0.00	0.00	13.46	0.00	0.00
Cellobiohydrolase	24.53	17.79	10.67	2.54	25.73	25.50	11.92	0.93	8.69	4.32	0.14	10.87	0.80	0.00
β-glucosidase	639.32 ab	531.88 a	423.21 ab	121.99 b	665.39 a	588.06 a	199.49 b	41.87 a	422.51 b	173.04 ab	101.17 ab	472.73	183.90	93.71
Exochitinase	52.35	68.15	33.55	19.32	42.98	37.19	17.02	22.63	56.83	16.46	17.04	48.41	15.32	16.73
Acid phosphatase	2512.58 a ϕ	583.71 ab	342.44 ab	225.56 b	621.07	437.00	220.81	131.68 ϕ	663.93	262.11	189.77	726.16	262.41	228.75
Phosphodiesterase	125.38 a	24.09 ab	14.01 b	12.75 b	31.18	19.31	10.45	12.32	40.75	10.94	7.54	40.46	11.67	7.84
Arylsulfatase	448.21 a	−	14.14 ab	63.79 ab	−	−	97.27	731.70 a	−	106.59 ab	16.75 ab	−	−	59.09
β-xylosidase	52.49 ab	34.94 a	12.53 b	16.70 b	37.41 a	19.59 b	14.22 b	25.05 ab	35.51 a	12.45 b	19.15 ab	34.51 a	10.65 b	15.36 ab

interactions amongst wood decay fungi and the rates at which they occur are affected by temperature (Schoeman et al., 1996; Hiscox and Boddy, 2017), and the changes in VOC emissions may be a consequence of, or even causal in, these changes. However, in the present study, increased production of some compounds, including 2,7-dimethyloctane (C55) an iso-branched *n*-alkane that is readily degraded by some fungal and bacterial strains (Schaeffer et al., 1979), also occurred in self-pairing controls, indicating temperature induced changes to innate metabolic processes as well. It is possible that the change in metabolic activities under the different conditions may be a direct or indirect cause of changes to the combative abilities of fungi, thus affecting the outcome and supporting the first study hypothesis.

However, in some cases interaction outcome did not appear to be closely correlated with enzyme and VOC activity. For example, the final outcome of interaction between *T. versicolor* versus *H. fasciculare* was deadlock both at 25 °C and in the field, but the activity of acid phosphatase, α-glucosidase, exochitinase and β-xylosidase, and the suite and abundance of VOCs were significantly different between the two environmental conditions. This would suggest that interaction outcomes are not the sole cause or effect of diverging metabolite profiles, and that the environment may be having a more direct effect on metabolic processes. Furthermore, in the natural environment fungi frequently interact simultaneously with several different species. Recent studies with three species of wood decay fungi interacting simultaneously revealed that the relative position of individuals within an interaction affects interaction outcomes (Hiscox et al. 2017, 2018; O'Leary et al., 2018). So while the present study provides valuable information regarding the relationship between interaction outcomes and metabolic processes, it is important to remember that in nature metabolic mechanisms will be even more complex.

4.2. Terminal hydrolase enzyme activity is greatest during deadlock, but enzyme activity generating reactive oxygen species is lower

When competitors are combatively unevenly matched, initially high levels of antagonistic compounds are deployed before one of the fungi successfully makes headway and begins the process of replacement (Hiscox and Boddy, 2017). The successful antagonist then utilises the mycelium of the displaced competitor and enzymes functioning in the breakdown of mycelia increase in the region of displacement (Hiscox and Boddy, 2017). This was seen in the present study where activity of enzymes throughout the course of the interaction between *T. versicolor* and *H. fasciculare* was generally highest soon after the interaction began, then decreased throughout the remainder of the experiment. Activities of some enzymes were highest after 14 d in the *H. fasiculare* block interaction zone, reflecting the start of the gradual replacement of *T. versicolor* by *H. fasciculare* after 14 d, then returned to pre-interaction levels. Mycelial damage is linked to the oxidative activities of reactive oxygen species (ROS) produced by enzymes such as laccase, peroxidases and NADPH oxidase (Hiscox and Boddy, 2017), however, while in the present study laccase production was significantly higher in the *T. versicolor* pre-colonised block following territory loss, peroxidase and MnP were not. Additionally, although interactions with *H. fasciculare* and *P. velutina* sometimes resulted in replacement of *T. versicolor* and sometimes in deadlock, changes in the activity of ROS-generating enzymes amongst interactions with different outcomes only occurred in the interaction with *P. velutina* at 15 °C, where laccase and MnP production decreased during deadlock compared with partial replacement of *T. versicolor*. This suggests that these enzymes are not always determinants of interaction outcome, and that other metabolic processes are occurring.

4.3. Decomposition processes are not solely affected by climate

Temperature had little effect on the rate of decomposition. However, changing temperatures form the basis of many global change projection models (IPCC, 2013), yet our results suggest that temperature may not be the predominant factor affecting fungal driven ecosystem processes. Furthermore, other factors such as water availability are also likely to play important roles in climate effects on fungal driven processes (Venugopal et al., 2016). Under different temperatures, however, individual combative success was altered which resulted in changes to the dominant species present and was reflected in the quantities of lignin and cellulose decomposing enzymes (supporting hypothesis 2), and thus, other factors such as community succession and individual life history strategies should be considered when predicting climate change effects. It would seem then that the decomposition of organic matter may be indirectly affected by changing temperatures via alterations to the suite of decomposition agents within the community, as well as by direct effects of temperature on metabolism.

4.4. In contrast to VOC profiles, enzymes function independently from each other

It is well known that VOCs function synergistically as a profile of compounds (Pennerman et al., 2016). For example, sesquiterpenes, and structurally diverse sesquiterpenoids, are produced in their thousands by bacteria, fungi and plants (Schmidt-Dannert, 2015) and, as in the present study, production of groups of sesquiterpenes often increases during interspecific interactions (Hynes et al., 2007). In the present study, production of the sesquiterpenes β-chamigrene (C58) and cedrene (C38), which have antifungal activity against *T. versicolor* and *Gloeohyllum trabeum* (Mun and Prewitt, 2011), increased during the interaction between *T. versicolor* and *C. puteana* at 15 °C when *T. versicolor* fully replaced its competitor (i.e. 28 d after the start of the interaction). This suggests production of the antimicrobial compounds by *T. versicolor* to gain and maintain territory, likely accompanied by a suite of defence mechanism compounds protecting it from its own antifungal production (Hiscox and Boddy, 2017). It is known that *Fagus sylvatica* produces its own suite of terpene classes (Tollsten and Müller, 1996) and that many decay fungi are enriched with secondary metabolite gene clusters, in particular, terpene synthases (Riley et al., 2014). An interesting consideration is the possibility that either some or all of the sesquiterpenes produced in this study are in fact plant derived, following a strategy of alteration of the plant-derived products by tailoring enzymes of the fungi for their own antagonistic advantage.

Enzymes were found to function independently of each other. It is possible that the full suite of complementary enzymes was not targeted within the study assays, thus the lack of discriminating profiles between sample groups, however, individual enzyme activity was significantly related to abiotic condition and interaction outcomes. It would seem then, that while the mechanisms of functionality for VOCs and extracellular enzymes contrast with each other, their production and activity are similarly linked to interaction outcome and environmental condition (hypothesis 1).

5. Conclusions

It has been reported previously that temperature causes interaction outcomes to change (Hiscox et al., 2016) and that competition changes the bouquet of VOCs (Hynes et al., 2007; Evans et al., 2008; El Ariebi et al., 2016), but the present study is novel in its

finding that metabolism is linked to changes in outcomes between wood decay fungi. Furthermore, tracking terminal hydrolase activity throughout the interaction between *T. versicolor* and *H. fasciculare*, revealed that its activity was greatest during deadlock and then returned to pre-interaction levels when *H. fasciculare* started the process of replacement of *T. versicolor* and territory occupation changed. While differences in enzyme and VOC profiles between interactions with different outcomes may be incidental, fewer compounds were produced when temperature was higher suggesting that they are directly affected by temperature. Since both enzymes and VOCs contribute to diverging combative abilities and outcomes through antimicrobial activities, the relationship between metabolite production and interaction outcome under different environmental regimes is most likely explained as: temperature directly affects the production of enzymes and VOCs, and the change in metabolite production mediates interaction outcomes. This scenario explains the vital role of fungal metabolism to forest ecosystem dynamics under environmental change, and supports the first study hypothesis that the link between metabolism and interaction outcome is affected by environmental conditions. It should be mentioned, however, that enzyme activity sometimes differed between identical pairings whose interaction outcome was the same under different environmental conditions, suggesting that interaction outcomes may not be the sole cause or effect of diverging metabolic profiles.

Authorship statement

LB, DCE, JH, CTM and HJR designed the experiment, LB, JH and MS set up the experiment, JO'L and CTM analysed VOCs, JH, AL, SWM and MS analysed enzymes, JO'L analysed the data and drafted the paper, and LB, DCE, JH, CTM and HJR contributed to writing and editing the paper. We have not been able to contact AL during paper writing, despite attempts via email and social media.

Acknowledgements

Supplementary data

Supplementary data to this article can be found online at https://doi.org/10.1016/j.funeco.2019.03.006.

References

Ahearn, D.G., Crow, S.A., Simmons, R.B., Price, D.L., Mishra, S.K., Pierson, D.L., 1997. Fungal colonisation of air filters and insulation in a multi-story office building: production of volatile organics. Curr. Microbiol. 35 (5), 305–308.
Allison, S.D., Treseder, K.K., 2008. Warming and drying suppress microbial activity and carbon cycling in boreal forest soils. Glob. Chang. Biol. 14 (12), 2898–2909.
Anderson, M.J., Willis, T.J., 2003. Canonical analysis of principle coordinates: a useful method of constrained ordination for ecology. Ecology 84, 511–525.
Baldrian, P., 2009. Microbial enzyme-catalyzed processes in soils and their analysis. Plant Soil Environ. 55 (9), 370–378.
Baldrian, P., Šnajdr, J., Merhautová, V., Dobiášová, P., Cajthaml, T., Valášková, V., 2013. Responses of the extracellular enzyme activities in hardwood forest to soil temperature and seasonality and the potential effects of climate change. Soil Biol. Biochem. 56, 60–68.
Benjamini, Y., Hochberg, Y., 1995. Controlling the false discovery rate – a practical and powerful approach to multiple testing. J. R. Stat. Ser. Soc. B Stat. Methodol. 57, 289–300.
Boddy, L., 2000. Interspecific combative interactions between wood-decaying basidiomycetes. FEMS Microbiol. Ecol. 31 (3), 185–194.
Boddy, L., 2001. Fungal community decomposition processes in angiosperms: from standing tree to complete decay of coarse woody debris. Ecol. Bull. 49, 43–56.
Borjesson, T., Stollman, U., Adamek, P., Kaspersson, A., 1989. Analysis of volatile compounds for detection of molds in stored cereals. Am Assoc Cereal Chem 66 (4), 300–304.
Bourbonnais, R., Paice, M.G., 1990. Oxidation of non-phenolic substrates. An expanded role for laccase in lignin biodegradation. FEBS Lett. 267, 99–102.
Chen, W.P., Liu, L.L., Yang, Y.Q., 1989. Synthesis and antifungal activity of N-(6,6-dimethyl-2-hepten-4-ynyl)-N-methyl-alpha-substituted -1-(4-substi tuted) naphthalenemethanamines. Acta Pharm. Sin. B 24 (12), 895–905.
Cordero, P., Principe, A., Jofre, E., Mori, G., Fischer, S., 2015. Inhibition of the phytopathogenic fungus *Fusarium proliferatum* by volatile compounds produced by *Pseudomonas*. Arch Microbiol 196 (11), 803–809.
Cox, P.M., Betts, R.A., Jones, C.D., Spall, S.A., Totterdell, I.J., 2000. Acceleration of global warming due to carbon-cycle feedbacks in a coupled climate model. Nature 408, 184–187.
Crowther, T., Jones, T.H., Boddy, L., Baldrian, P., 2011. Invertebrate grazing determines enzyme production by basidiomycete fungi. Soil Biol. Biochem. 42, 2060–2068.
Davidson, E.A., Janssens, I.A., 2006. Temperature sensitivity of soil carbon decomposition and feedbacks to climate change. Nature 440, 165–173.
Eichlerová, I., Homolka, L., Žifčáková, L., Lisá, L., Dobiášová, P., Baldrian, P., 2015. Enzymatic systems involved in decomposition reflects ecology and taxonomy of saprotrophic fungi. Fungal Ecol 13, 10–22.
El Ariebi, N., Hiscox, J., Scriven, S.A., Müller, C.T., Boddy, L., 2016. Production and effects of volatile organic compounds during interspecific interactions. Fungal Ecol 20, 144–154.
Evans, J., Eyre, C.A., Rogers, H.J., Boddy, L., Müller, C.T., 2008. Changes in volatile production during interspecific interactions between four wood rotting fungi growing in artificial media. Fungal Ecol 1, 57–68.
Fawcett, R., Collins-George, N., 1967. A filter-paper method for determining the moisture characteristics of soil. Aust. J. Exp. Agric. Anim. Husb. 7, 162–167.
Fernandez de Simon, B., Sanz, M., Cadahia, E., Esteruelas, E., Minoz, A.M., 2014. Nontargeted GC–MS approach for volatile profile of toasting in cherry, chestnut, false acacia, and ash wood. J. Mass Spectrom. 49 (5), 353–370.
Geethalakshmi, R., Sarada, D.V.L., 2013. Evaluation of antimicrobial and antioxidant activity of essential oil of *Trianthema decandra L*. J. Pharm. Pharm. Sci. 6 (1), 101–106.
Gutierrez, A., del Rio, J.C., Martinez-Inigo, M., Martinez, M.J., Martinez, A.T., 2002. Production of new unsaturated lipids during wood decay by ligninolytic basidiomycetes. Appl. Environ. Microbiol. 68 (3), 1344–1350.
Hansen, J., Ruedy, R., Sato, M., Lo, K., 2006. GISS surface temperature analysis. Global Temperature Trends: 2005 Summation. NASA Goddard Institute for Space Studies and Columbia University Earth Institute, New York.
Hiscox, J., Boddy, L., 2017. Armed and dangerous – chemical warfare in wood decay communities. Fungal Biol Rev 31, 169–184.
Hiscox, J., Baldrian, P., Rogers, H.J., Boddy, L., 2010. Changes in oxidative enzyme activity during interspecific mycelial interactions involving the white-rot fungus *Trametes versicolor*. Fungal Genet. Biol. 47, 562–571.
Hiscox, J., Clarkson, G., Savoury, M., Powell, G., Savva, I., Lloyd, M., Shipcott, J., Choimes, A., Cumbriu, X.A., Boddy, L., 2016. Effects of pre-colonisation and temperature on interspecific fungal interactions in wood. Fungal Ecol 21, 32–42.
Hiscox, J., O'Leary, J., Boddy, L., 2018. Fungus wars: basidiomycete battles in wood decay. Stud. Mycol. 89, 117–124.
Hiscox, J., Savoury, M., Toledo, S., Kingscott-Edmunds, J., Bettridge, A., Al Waili, N., Boddy, L., 2017. Threesomes destabilise certain relationships: multispecies interactions between wood decay fungi in natural resources. FEMS Microbiol. Ecol. 93 https://doi.org/10.1093/femsec/fix014.
Ho, C.L., Liao, P.C., Hsu, K.P., Wang, E.I., Dong, W.C., Su, Y.C., 2010. Composition and antimicrobial and anti-wood-decay fungal activities of the leaf essential oils of *Machilus pseudolongifolia* from Taiwan. Nat Prod Commun 5 (7), 1143–1146.
Hynes, J., Müller, C., Jones, H.T., Boddy, L., 2007. Changes in volatile production during the course of fungal mycelial interactions between *Hypholoma fasciculare* and *Resinicium bicolor*. J. Chem. Ecol. 33, 43–57.
IPCC, 2007. Climate change 2007: the physical science basis. In: Solomon, S., Qin, D., Manning, M., Chen, Z., Marquis, M., Averyt, K.B., Tignor, M., Miller, H.L. (Eds.), Contribution of Working Group I to the Fourth Assessment Report of the Intergovernmental Panel on Climate Change. Cambridge University Press, Cambridge, pp. 847–996.
IPCC, 2013. Climate change 2013: the physical science basis. In: Stocker, T.F., Qin, D., Plattner, G.K., Tignor, M., Allen, S.K., Boschung, J., Nausels, A., Xia, Y., Bex, V., Midgley, P.M. (Eds.), Contribution of Working Group I to the Fourth Assessment Report of the Intergovernmental Panel on Climate Change. Cambridge University Press, Cambridge, pp. 1029–1136.
Isidorov, V., Tyszkiewicz, Z., Piroznikow, E., 2016. Fungal succession in relation to volatile organic compounds emissions from Scots pine and Norway spruce leaf litter-decomposing fungi. Atmos. Environ. 131, 301–306.
Kindt, R., Coe, R., 2005. Tree diversity analysis. A Manual and Software for Common Statistical Methods for Ecological and Biodiversity Studies. World Agroforestry Centre, Nairobi.
Konayli, S., Ocak, M., Aliyazicioglu, R., Karaoglu, S., 2009. Chemical analysis and biological activities of essential oils from trunk-barks of eight trees. Asian J. Chem. 21, 2684–2694.
Kong, C., Xu, X., Zhou, B., Hu, F., Zhang, C., Zhang, M., 2004. Two compounds from allelopathic rice accession and their inhibitory activity on weeds and fungal pathogens. Phytochemistry 65 (8), 1123–1128.
Konuma, R., Umezawa, K., Mizukoshi, A., Kawarada, K., Yoshida, M., 2015. Analysis of

microbial volatile organic compounds produced by wood-decay fungi. Biotechnol. Lett. 37 (9), 1845—1852.

Langfelder, P., Horvath, S., 2012. Fast R functions for robust correlations and hierarchical clustering. J. Stat. Softw. 46 (11), 1—17.

Liouane, K., Saidana, D., Edziri, H., Ammar, S., Chriaa, J., Mahjoub, M.A., Said, K., Mighri, Z., 2010. Chemical composition and antimicrobial activity of extracts from Gliocladium sp. growing wild in Tunisia. Med. Chem. Res. 19 (8), 743—756.

Lippolis, V., Pascale, M., Cervellieri, S., Damascelli, A., Visconti, A., 2014. Screening of deoxynivalenol contamination in durum wheat by MOS-based electronic nose and identification of the relevant pattern of volatile compounds. Food Control 37, 263—271.

Maynard, D.S., Crowther, T.W., Bradford, M.A., 2017. Competitive network determines the direction of the diversity-function relationship. Proc Nat Sci Acad USA 114 (43). https://doi.org/10.1073/pnas.1712211114.

Micheluz, A., Manente, S., Rovea, M., Slanzi, D., Varese, G.C., Ravagnan, G., 2016. Detection of volatile metabolites of moulds isolated from a contaminated library. J. Microbiol. Methods 128, 34—41.

Moody, S.C., Dudley, E., Hiscox, J., Boddy, L., Eastwood, D.C., 2018. Inter-dependence between primary metabolism and xenobiotic mitigation characterises the proteome of Bjerkandera adusta decomposing wood. Appl. Environ. Microbiol. 84 (2), e01401—e01417.

Mun, A.P., Prewitt, L., 2011. Antifungal activity of organic extracts from Juniperus virginiana heartwood against wood decay fungi. For. Prod. J. 61 (6), 443—449.

O'Leary, J., Eastwood, D., Müller, C., Boddy, L., 2018. Emergent properties arising from spatial heterogeneity influence community dynamics. Fungal Ecol 33, 32—39.

Oksanen, J., Blanchet, F.G., Kindt, R., Legendre, P., Minchin, P.R., O'Hara, R.B., Simpson, G.L., Solymos, P., Stevens, M.H.H., Wagner, H., 2013. Vegan: community ecology package. R Package Version 2, pp. 0—8.

Pan, Z., Jin, S., Zhang, X., Zheng, S., Han, S., Pan, L., Lin, Y., 2016. Biocatalytic behavior of a new Aspergillus niger whole-cell biocatalyst with high operational stability during the synthesis of green biosolvent isopropyl esters. J. Mol. Catal. B Enzym. 131, 10—17.

Pennerman, K.K., Al-Maliki, H.S., Bennett, J.W., 2016. Fungal volatile organic compounds (VOCs) and the genus Aspergillus. In: Gupta, V.K. (Ed.), New and Future Developments in Microbial Biotechnology and Bioengineering. Elsevier, Amsterdam, pp. 95—115.

Pernak, J., Zabielska-Matejuk, J., Kropacz, A., Foksowicz-Flaczyk, J., 2004. Ionic liquids in wood preservation. Holzforschung 58 (3). https://doi.org/10.1515/HF.2004.044.

Post, W.M., Emanuel, W.R., Zinke, P.J., Stangenberger, A.G., 1982. Soil carbon pool and world life zones. Nature 298, 156—159.

Qadri, M., Nalli, Y., Jain, S.K., Chaubey, A., Ali, A., Strobel, G.A., Vishwakarma, R.A., Riyaz-Ul-Hassan, S., 2017. An insight into the secondary metabolism of Muscodor yucatanesis: small-molecule epigenetic modifiers induce expression of secondary metabolism-related genes and production of mew metabolites in the endophyte. Microb. Ecol. 73 (4), 954—965.

R Core Team, 2014. R: a Language and Environment for Statistical Computing. R Foundation for Statistical Computing, Vienna. http://www.R-project.org/.

Riley, R., Salamova, A.A., Brown, D.W., Nagy, L.G., Floudas, D., Heldd, B.W., Levasseur, A., Lombard, V., Morin, E., Otillar, R., Lindquist, E.A., Sun, H., LaButti, K.M., Schmutz, J., Jabbour, D., Luo, H., Baker, S.E., Pisabarro, A.G., Walton, J.D., Blanchette, R.A., Henrissat, B., Martin, F., Cullen, D., Hibbett, D.S., Grigoriev, I.V., 2014. Extensive sampling of basidiomycete genomes demonstrates inadequacy of the white-rot/brown-rot paradigm for wood decay fungi. Proc Nat Sci Acad USA 111 (27), 9923—9928.

Rivas da Silva, A.C., Lopes, P.M., Barros de Azevedo, M.M., Costa, D.C.M., Alviano, C.S., Alviano, D.S., 2012. Biolgical activities of á-pinene and β-pinene enantiomers. Molecules 17, 6305—6316.

Sánchez-Fernández, R.E., Diaz, D., Duarte, G., Lappe-Oliveras, P., Sanchez, S., Macias-Rubalcava, M.L., 2016. Antifungal volatile organic compounds from the endophyte nodulisporium sp. strain GS4d2II1a: a qualitative change in the intraspecific and interspecific interactions with Pythium aphanidermatum. Microb. Ecol. 71 (2), 347—364.

Savel'eva, E.I., Gavrilova, O.P., Gagkaeva, Y.Y., 2014. Study of the composition of volatile organic compounds emitted by the filamentous fungus Fusarium culmorum by gas chromatography-mass spectrometry combined with solid phase microextraction. Russ. J. Gen. Chem. 84 (13), 2603—2610.

Schaeffer, T.L., Cantwell, S.G., Brown, J.L., Watt, D.S., Fall, R.R., 1979. Microbial growth on hydrocarbons: terminal branching inhibits biodegradation. Appl. Environ. Microbiol. 38 (4), 742—746.

Schalchli, H., Hormazabal, E., Becerra, J., Birkett, M., Alvear, M., Vidal, J., Quiroz, A., 2011. Antifungal activity of volatile metabolites emitted by mycelial cultures of saprophytic fungi. Chem. Ecol. 27 (6), 503—513.

Schmidt-Dannert, C., 2015. Biosynesthsis of terpenoid natural products in fungi. In: Schrader, J., Bohlmann, J. (Eds.), Biotechnology of Isoprenoids. Advances in Biochemical Engineering/Biotechnology. Springer, New York, pp. 19—62.

Schoeman, M.W., Webber, J.F., Dickinson, D.J., 1996. The effect of diffusible metabolites of Trichoderma harzianum on in vitro interactions between basidiomycete isolates at two different temperature regimes. Mycol. Res. 100, 1454—1458.

Sen, S., Dehingia, M., Talukdar, N.C., Khan, M., 2017. Chemometric analysis reveals links in the formation of fragrant bio-molecules during agarwood (Aquilaria malaccensis) and fungal interactions. Sci. Rep. 7 https://doi.org/10.1038/srep44406.

Sharip, N.S., Ariffin, H., Hassan, M.A., Nishida, H., Shirai, Y., 2016. Characterization and application of bioactive compounds in oil palm mesocarp fiber superheated steam condensate as an antifungal agent. Railw. Syst. Controls 6, 84672—84683.

Sinha, M., Sorensen, A., Ahamed, A., Ahring, K., 2015. Production of hydrocarbons by Aspergillus carbonarius ITEM 5010. Fungal Biol 119 (4), 274—282.

Šnajdr, J., Dobiášová, P., Vetrovský, T., Valášková, V., Alawi, A., Boddy, L., Baldrian, P., 2011. Saprotrophic basidiomycete mycelia and their interspecific interactions affect the spatial distribution of extracellular enzymes in soil. FEMS Microbiol. Ecol. 78 (1), 80—90.

Stein, S.E., 2011. National Institute of Standards and Technology Library Software Version 2.0 G. Available at: https://www.nist.gov/sites/default/files/documents/srd/NIST1a11Ver2-0Man.pdf.

Sun, D., Meng, J., Liang, H., Yang, E., Huang, Y., Chen, W., Jiang, L., Lan, Y., Zhang, W., Gao, J., 2015. Effect of volatile organic compounds absorbed to fresh biochar on survival of Bacillus mucilaginosus and structure of soil microbial communities. J. Soils Sediments 15 (2), 271—281.

Suwannarach, N., Bussaban, B., Nuangmek, W., Pithakpol, W., Jirawattanakul, B., Matsui, K., Lumyong, S., 2016. Evaluation of Muscodor suthepensis strain CMU-Cib462 as a postharvest biofumigant for tangerine fruit rot caused by Penicillium digitatum. J Sci Food Agric 96 (1), 339—345.

Toljander, Y.K., Lindahl, B.J.D., Holmer, L., Högberg, N.O.S., 2006. Environmental fluctuations facilitate species co-existence and increase decomposition in communities of wood decay fungi. Oecologia 148, 625—631.

Tollsten, L., Müller, P.M., 1996. Volatile organic compounds emitted from beech leaves. Phytochemistry 43 (4), 759—762.

Usha Nandhini, S., Sangareshwari, S., Kumari, L., 2015. Gas chromatography-mass spectrometry analysis of bioactive constituents from the marine Streptomyces. Asian J. Pharmaceut. Clin. Res. 8 (2), 0974—2441.

Venugopal, P., Junninen, K., Linnakoski, R., Edman, M., Kouki, J., 2016. Climate and wood quality have decayer-specific effects on fungal wood decomposition. For. Ecol. Manag. 360, 341—351.

White, N., 2003. The importance of wood-decay fungi in forest ecosystems. In: Arora, D.K., Bridge, P.D., Bhatnagar, D. (Eds.), Fungal Biotechnology in Agricultural, Food and Environmental Applications. Marcel Dekker, New York. https://doi.org/10.1201/9780203913369.ch32.

Wihlborg, R., Pippitt, D., Marsili, R., 2016. Headspace sorptive extraction and GC-TOFMS for the identification of volatile fungal metabolites. J. Microbiol. Methods 75 (2), 244—250.

Xia, J., Wishart, D.S., 2015. Using MetaboAnalyst 3.0 for comprehensive metabolomics data analysis current protocols in bioinformatics. Curr Protoc Bioinformatics 55, 14, 10.1-14.10.91.

Yan, C., Yu, J.X., Xing, T., Qing, C.X., 2008. Comparison of volatile components from Marchantia convolute obtained by microwaves extraction and phytosol extraction. J. Chil. Chem. Soc. 53 (2), 1518—1522.

Zerinque, H.J., Bhatnagar, D., 1994. Effects of neem leaf volatiles on submerged cultures of aflatoxigenic Aspergillus parasiticus. Appl. Environ. Microbiol. 60 (10), 3543—3547.